EPSC Abstracts
Vol. 13, EPSC-DPS2019-193-1, 2019
EPSC-DPS Joint Meeting 2019

EPSC
EPSC-DPS Joint Meeting 2019
15–20 September 2019 | Geneva, Switzerland

Photochemical model of Pluto's atmosphere and ionosphere

Vladimir A. Krasnopolsky
Moscow Institute of Physics and Technology (PhysTech), Russia (vlad.krasn@verizon.net)

Abstract

This is a self-consistent model of Pluto's photochemistry that involves 83 neutral and 35 ion species up to the exobase at 1600 km with vertical transport by eddy, molecular, and ambipolar diffusion. The model agrees with the New Horizons and ALMA observations and does not require revision of the laboratory data on the C_2H_4 and C_2H_6 vapor pressure. Evolution of the atmosphere by thermal escape, condensation and polymerization of photochemical products is discussed.

1. Introduction

The New Horizons flyby of Pluto [1,2,8] along with the ALMA [5] and VLT/CRIRES [4] high-resolution spectroscopy and the recent stellar occultations resulted in significant progress in Pluto's atmosphere. These new data require updated photochemical modelling. The model by Wong et al. [7] includes detailed neutral chemistry at 40 levels up to 1300 km. To fit the observations, the authors adopted saturated vapor densities of C_2H_4 and C_2H_6 equal to those of C_2H_2, though they differ by orders of magnitude. Here we present a model that does not require the revision of the laboratory data on the saturated vapor densities and involves ion chemistry that affects the neutral composition and is missing in Wong et al. [7].

2. Model

The model by Krasnopolsky [3] that reproduces fairy well the observed properties of Titan's atmosphere and ionosphere is adjusted to the conditions of Pluto during the New Horizons flyby. It involves 83 neutrals and 35 ions and extends up to the exobase at 1600 km. Thermal escape of neutrals and diffusion of ions are the upper boundary conditions. Condensation on the haze and surface are the lower boundary conditions.

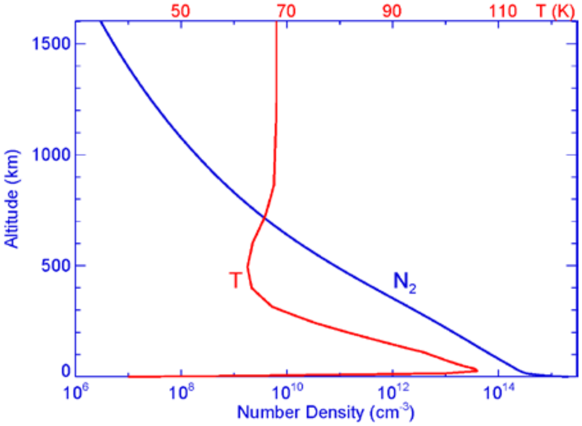

Fig. 1. The observed temperature and calculated N_2 density profiles

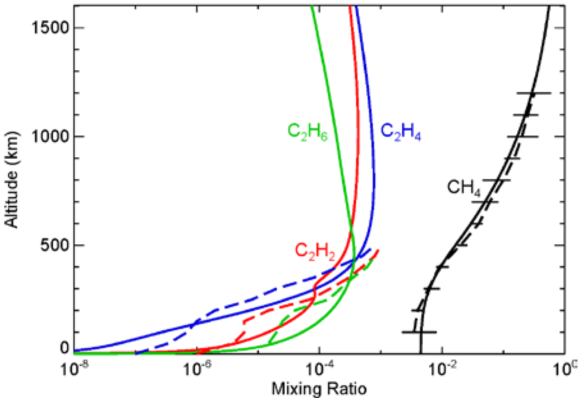

Fig. 2. Observed (dashed curves) and calculated (solid curves) profiles of the main hydrocarbons

3. Model results

The adopted eddy diffusion $K = 3\times10^4$ cm^2 s^{-1} facilitates transport and condensation of C_2H_6 on the surface (Fig. 2) and does not require the revision of the laboratory data on the saturated vapor densities. The CH_4 homopause is at 90 km for this *K*, and the CH_4 profile is mostly controlled by molecular diffusion and agrees with the observations (Fig. 2).

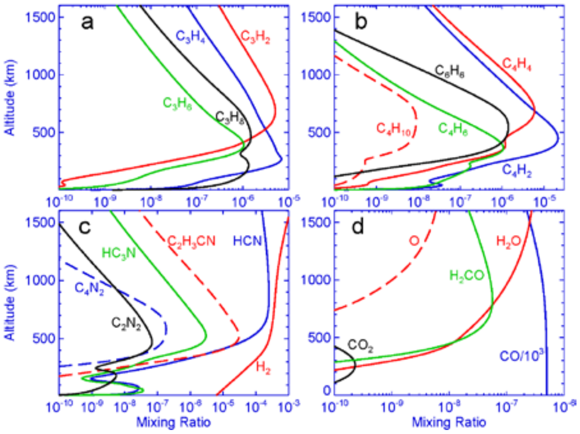

Fig. 3. Vertical profiles of C_3 hydrocarbons (*a*), C_4 hydrocarbons and benzene (*b*), nitriles and H_2 (*c*), and oxygen species (*d*)

Major production and loss processes of the observed species are briefly discussed. Ion chemistry significantly contributes to those. The most abundant C_3, C_4 hydrocarbons and benzene are shown in Fig. 3a, b. Diacetylene C_4H_2 is effective in polymerization with C_6H and C_3N. Sticking coefficients for condensation of hydrocarbons and nitriles are adopted at 0.002 and 0.01, respectively.

Some nitriles and H_2 are depicted in Fig. 3c. The HCN abundance agrees with the ALMA [5] observations. The HC_3N warm layer below 150 km constitutes 90% of its column abundance and is weakly sensitive to the adopted sticking and slightly exceeds the observed upper limit.

H and H_2 are formed by photolysis of hydrocarbons. 60% of the production of H escape, and the remaining 40% react with radicals and form H_2, Almost all H_2 escapes. Its mole fraction increases up to 400 km due to diffusive separation. Further increase reflects a balance between the production and escape.

Oxygen chemistry (Fig. 3d) is stimulated by CO and the meteorite H_2O that is very weak, according to the interplanetary dust dynamic model [6].

Ionosphere is formed by the solar EUV ionization and the galactic cosmic rays that dominate below 300 km (Fig. 4). The ionospheric peak is at 750 and 850 km with e_{max} = 800 and 300 cm^{-3} on the day side and near the terminator, respectively. It agrees with the New Horizons upper limit of 1000 cm^{-3}. The heavy ion $C_9H_{11}^+$ is the most abundant below 650 km (Fig. 4a). The main ions above 650 km are $HCNH^+$, $C_2H_5^+$, and $C_3H_5^+$. The predicted ion densities are well within the range of the Cassini Ion-Neutral Mass Spectrometer.

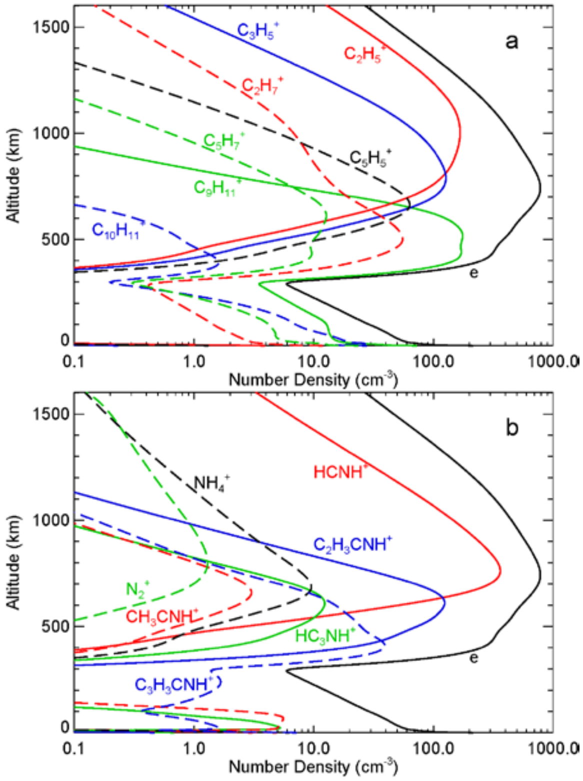

Fig. 4. The most abundant hydrocarbon (*a*) and nitrogen-bearing (*b*) ions

Evolution: The calculated annual mean rates are 150 g cm^{-2} Byr^{-1} for escape of CH_4 + CH_3 and H_2 + H, 150 and 50 g cm^{-2} Byr^{-1} for precipitation of hydrocarbons and nitriles, respectively. The surface is young, and the surface mixing is significant.

Pluto and Triton: The great differences (by orders of magnitude) between the atmospheres and ionospheres of Pluto and Triton are caused by the methane abundances. Transition from Triton's conditions observed in the Voyager flyby to Pluto's conditions in the New Horizons flyby is expected near $CH_4 \approx 0.05\%$. Both Triton and Pluto undergo these transitions during their annual cycles.

References

[1] Gladstone G.R. et al. Science 351, aad8866, 2016
[2] Hinson D.P. et al. Icarus 290, 96-111, 2017
[3] Krasnopolsky V.A. Icarus 236, 83-91, 2014
[4] Lellouch E. et al. Astron. Astrophys. 530, L4, 2011
[5] Lellouch E. et al. Icarus 286, 289-307, 2017
[6] Poppe A.R. and Horanyi M. Astron. Astrophys. 617, L5, 2018
[7] Wong M.L. et al. Icarus 287, 110-115, 2017
[8] Young L.A. et al. Icarus 300, 174-199, 2018